

# The Role of Phosphate Binding in Purine Nucleoside Phosphorylase of *Helicobacter pylori*

Marta Bošnjaković, Ivana Leščić Ašler, Zoran Štefanić\*

Division of Physical Chemistry, Ruđer Bošković Institute, POB 180, HR-10002 Zagreb, Croatia

\* Corresponding author's e-mail address: zoran.stefanic@irb.hr

RECEIVED: April 6, 2018 \* REVISED: May 8, 2018 \* ACCEPTED: May 14, 2018

— THIS PAPER IS DEDICATED TO DR. BISERKA KOJIĆ-PRODIĆ ON THE OCCASION OF HER 80<sup>TH</sup> BIRTHDAY —

**Abstract:** Purine nucleoside phosphorylase (PNP) is an essential enzyme in the purine salvage pathway of *Helicobacter pylori*. Since *H. pylori* lacks the ability to synthesize purine nucleosides *de novo*, inhibition of this enzyme could stop the growth of this bacterium. However, for the design of successful inhibitors the details of the mechanism of this enzyme should be fully understood. PNPs catalyze cleavage of the glycosidic bond of purine nucleosides, and phosphate is one of the substrates. It is thought that binding of phosphate induces the conformational change as a necessary initial step in the catalysis. This conformational change is manifested in closing of either one of the six active sites in the homohexameric PNPs. It is unclear whether the binding of phosphate is sufficient or just a necessary condition for the closing of the active site. In this paper we conducted an experiment to check this by soaking the crystals of the apo form of the enzyme in increasing concentrations of phosphate.

**Keywords:** active site conformation, enzyme catalysis, purine nucleoside phosphorylase, phosphate binding.

## INTRODUCTION

SUCCESSFUL design of enzyme inhibitors, and therefore also of prospective drugs, requires a detailed knowledge of their mechanism of action. This becomes even more important when the enzyme in question, purine nucleoside phosphorylase (PNP), is an attractive drug target from *Helicobacter pylori*, one of the pathogens that represents a very serious threat to human health.<sup>[1]</sup> Although much progress has been made over the years of our research on PNP from *E. coli*, the complete blueprint of the catalytic mechanism of PNP is yet to be drawn.<sup>[2–8]</sup> What makes PNP an attractive target for the fight against this severe pathogen is the fact that this bacterium relies exclusively on the purine salvage pathway for the synthesis of purine nucleosides, and in this pathway the PNP plays a key role.<sup>[9]</sup> For that reason inhibiting this enzyme would cut down the only source of nucleosides and ultimately would lead to its eradication.

The PNPs in bacteria are predominantly homohexamers, although there are also trimeric ones.<sup>[10]</sup> Each monomer in *H. pylori* is 237 amino acids in length.<sup>[5]</sup> Each

monomer pairs up with one of its neighbors by mutually completing the active sites with two amino acids (His4 and Arg43, Figure 1a). This pair of monomers forms a dimer via an approximate two-fold rotation symmetry. The complete hexamer is then formed by three-fold rotation of the dimers, thus making a hexamer with an approximate 32 point group symmetry (Figure 1b).

The reaction that PNP catalyzes is the cleavage of the glycosidic bond of purine (2'-deoxy)nucleosides, leading to free base and (2'-deoxy)ribose-1-phosphate as products. Therefore it requires phosphate as one of its substrates. In addition to its role as a substrate, phosphate also initiates the conformational change that is necessary for the catalysis. Namely, binding of phosphate induces a segmentation of the helix H8 located at the entrance to the active site.<sup>[2]</sup> The segmentation of the helix H8 occurs at the amino acid Phe221 and a smaller part of that helix moves towards the active site. This makes the active site less accessible from the outside and is known as closed conformation (Figure 2). The movement of the segmented part of the H8 helix is necessary to bring the side chain of the amino acid Arg217 in the vicinity of Asp204 and initiate

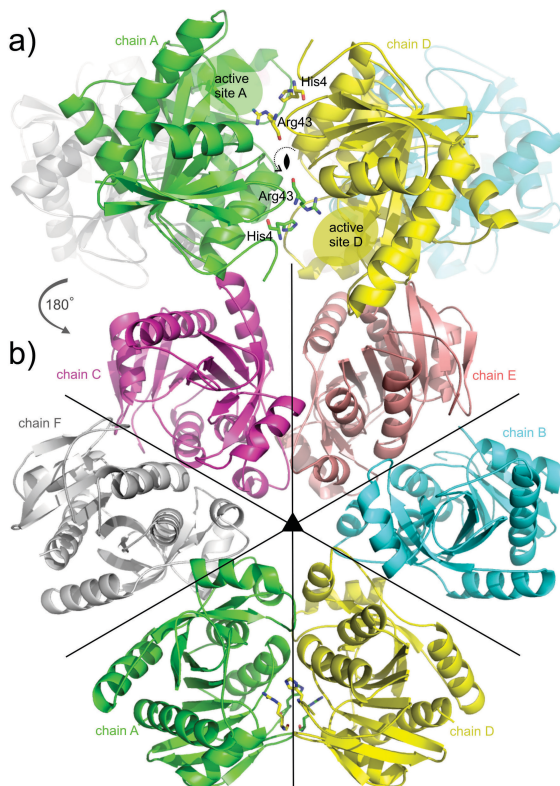


**Figure 1.** The overall architecture of the PNP from *H. pylori* hexamer (PDB code: 6G7X). a) Individual monomers join together to form dimers with two-fold symmetry axis. Each monomer completes the active site of the other monomer in the dimer by donating two amino acids, His4 and Arg43. b) Three such dimers are joined together by three-fold symmetry to form a full hexamer.

the catalysis.<sup>[6]</sup> This initial step in the catalysis has been confirmed by kinetic and mutation studies.<sup>[2]</sup>

However, the active sites in PNP do not open and close independently. Namely, closing of the active site is connected to other sites by negative cooperativity, which means that closing of one active site makes it more difficult for the other active sites to close.<sup>[6]</sup> The mechanism by which this cooperativity is realized is yet unclear. It is not known whether this occurs primarily between the monomers in a single dimer, or is it also the case between the monomers from different dimers. In a recent survey of various possible configurations of open and closed active sites in all the determined crystal structures of PNPs from different organisms, quite a number of possibilities was found,<sup>[8]</sup> and PNP from *H. pylori* even shows some previously unknown ones.<sup>[7]</sup>

In an attempt to isolate the event of phosphate binding to an apo form of PNP we have considered an experiment where all the spurious factors that could influence this binding are minimized. Specifically, to

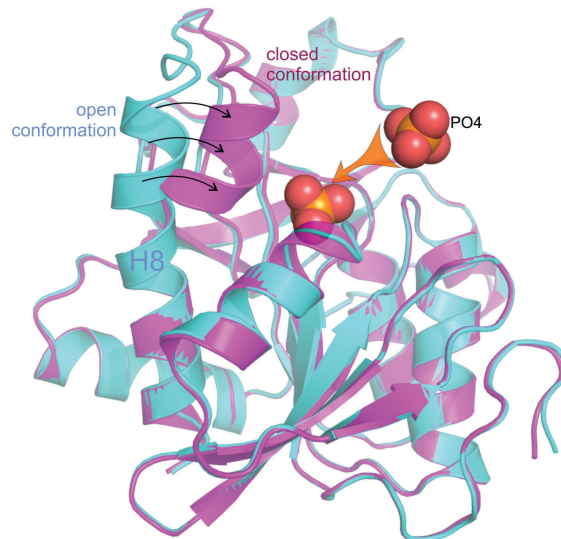


**Figure 2.** Overlap of the open and closed conformation of one monomer of PNP from *H. pylori* (PDB code: 5MX4).<sup>[5]</sup> It can be seen that majority of the monomer stays exactly the same, and the segmentation of the helix H8 partially closes the active site. The binding of phosphate and its position are drawn schematically.

eliminate all the different conditions that could affect the phosphate binding, the crystals of the apo form of the enzyme were soaked in different concentrations of phosphate. For this reason, this was done using the crystals from the very same crystallization drop. We have tried to scan wide range of phosphate concentrations (varying two orders in magnitude), trying not only to get binding of phosphate, but also to establish the order in which the active sites were populated.

## EXPERIMENTAL SECTION

### Cloning, Expression and Purification of PNP from *H. pylori*

*H. pylori* strain ATCC 26695 genomic DNA was obtained from the Department of Bacterial Genetics, Institute of Microbiology, Faculty of Biology, University of Warsaw. As described before for the PNP from clinical isolate of *H. pylori*,<sup>[5]</sup> *deoD* gene was cloned into pET21b expression vector (Invitrogen, Germany). The DNA sequence of *deoD* gene from *H. pylori* was confirmed by sequence analysis (Macrogen, Netherlands).

For the expression of PNP from *H. pylori* (HpPNP), the constructed plasmid pET21b-*HPdeoD* was subcloned into *E. coli* cell strain BL21-CodonPlus(DE3)-RIL (Agilent, US). The expression of PNP was performed essentially as described before.<sup>[8]</sup>

Two-step purification (anion exchange and affinity chromatography) of overexpressed protein was performed as described previously.<sup>[5]</sup> The activity assay using N(7)-methylguanosine as a substrate<sup>[5]</sup> and the protein concentration assay using the method of Bradford<sup>[11]</sup> with bovine serum albumin as a standard were used for following the purification procedure. For purified HpPNP, protein concentration was determined from UV spectra using the molar extinction coefficient (calculated from the amino acid sequence)<sup>[12]</sup> at 280 nm  $\epsilon = 13410 \text{ mol}^{-1} \text{ L cm}^{-1}$ . Protein purity was confirmed by SDS-PAGE on PhastSystem (GE Healthcare, UK) in 12.5 % acrylamide.

### Crystallization, Data Collection and Structure Determination

Crystals suitable for X-ray diffraction were grown in crystallization conditions containing 0.2 mol L<sup>-1</sup> imidazole, 40 % (w/v) polypropylene glycol (PPG) 400 and 0.02 % NaN<sub>3</sub>, pH = 7.0 (conditions B7 from MIDAS screen, Molecular dimensions, Newmarket, UK). Crystallization was carried out by means of a vapor diffusion method in a hanging drop setup, where the wells contained 700  $\mu\text{L}$  of the crystallization solution, and the drops contained 1  $\mu\text{L}$  of purified protein mixed with 1  $\mu\text{L}$  of crystallization solution. One series of crystallization contained 12 wells wherein the concentration of the PNP protein used was 11.61 mg mL<sup>-1</sup>. The second series of crystallization contained 8 wells wherein the concentration of the PNP used was 14.49 mg mL<sup>-1</sup>. Both plates were set up at 18 °C. For the soaking of crystals the solutions of phosphate in crystallization conditions were prepared. The final phosphate concentrations were: 100 mmol L<sup>-1</sup>, 50 mmol L<sup>-1</sup>, 25 mmol L<sup>-1</sup>, 12.5 mmol L<sup>-1</sup>, 6.25 mmol L<sup>-1</sup>, 3.125 mmol L<sup>-1</sup>, 1.56 mmol L<sup>-1</sup> and 0.78 mmol L<sup>-1</sup>.

Protein crystals were soaked in two ways. One way was to transfer the crystal from the crystallization drop to 0.5  $\mu\text{L}$  drop of phosphate solution, soak it for one minute and then freeze it in liquid nitrogen. The second way involved the addition of 0.5  $\mu\text{L}$  of phosphate solution to the original crystallization drop, starting with the lowest concentration and fishing one crystal one minute after each new addition. Data collection on around twenty crystals from different phosphate concentrations was done at the XRD1 beamline of the Elettra synchrotron, Trieste, Italy using the Dectris Pilatus 2M detector. The data collection and refinement parameters for the structure described here are summarized in Table 1. The data was integrated using the XDS program.<sup>[13]</sup> The structure was solved by molecular replacement using the Molrep program<sup>[14]</sup> and using the structure of HpPNP apo structure as a model (PDB code 6F52).<sup>[7]</sup> The refinement of the structure was carried out using the phenix.refine routine from the Phenix package.<sup>[15]</sup> The atomic coordinates and structure factors

**Table 1.** Data collection and refinement statistics for the monoclinic structure.

|                                |   |
|--------------------------------|---|
| Wavelength (Å)                 | 1.0                                     |
| Resolution range               | 46.7 – 1.8 (1.82 – 1.76) <sup>(a)</sup> |
| Space group                    | P2 <sub>1</sub>                         |
| <b>Unit cell</b>               |   |
| <i>a, b, c, (Å)</i>            | 93.3, 91.5, 93.4                        |
| $\beta$ (°)                    | 119.9                                   |
| Total reflections              | 829920                                  |
| Unique reflections             | 133850 (13061)                          |
| Multiplicity                   | 6.2                                     |
| Completeness (%)               | 99.7                                    |
| Mean I/sigma(I)                | 12.9                                    |
| Wilson B-factor                | 13.60                                   |
| <i>R</i> <sub>merge</sub>      | 0.09                                    |
| <b>Refinement</b>              |   |
| Reflections used in refinement | 133826 (13058)                          |
| Reflections used for R-free    | 1986 (186)                              |
| <i>R</i> <sub>work</sub>       | 0.15 (0.21)                             |
| <i>R</i> <sub>free</sub>       | 0.19 (0.25)                             |
| Number of non-hydrogen atoms   | 12053                                   |
| macromolecules                 | 10881                                   |
| ligands                        | 145                                     |
| Protein residues               | 1398                                    |
| RMS(bonds)                     | 0.029                                   |
| RMS(angles)                    | 0.81                                    |
| Ramachandran favoured (%)      | 96.8                                    |
| Ramachandran allowed (%)       | 3.2                                     |
| Ramachandran outliers (%)      | 0                                       |
| Rotamer outliers (%)           | 0.67                                    |
| Clash score                    | 4.76                                    |
| Average B-factor               | 18.97                                   |
| macromolecules                 | 18.03                                   |
| ligands                        | 31.10                                   |
| solvent                        | 27.16                                   |

<sup>(a)</sup> Values in parentheses refer to the highest resolution shell.

have been deposited in the Protein Data Bank: with accession code 6G7X.

## RESULTS AND DISCUSSION

Although more than twenty datasets were collected at the synchrotron beamline, only a single crystal structure was determined. Most of the crystals diffracted to satisfactory resolution of around 2–2.5 Å, but showed very high mosaicity, pseudo-symmetry and/or twinning related pathologies. It was very difficult to index the reflections and

to integrate the data. In few of the cases two space groups were identified: a triclinic one in the space group  $P\bar{1}$  with unit cell  $a = 93.3 \text{ \AA}$ ,  $b = 93.3 \text{ \AA}$ ,  $c = 95.3 \text{ \AA}$ ,  $\alpha = 92.6^\circ$ ,  $\beta = 97.9^\circ$  and  $\gamma = 120.1^\circ$ , and a monoclinic one in the space group  $C2$  with unit cell  $a = 162.1 \text{ \AA}$ ,  $b = 93.5 \text{ \AA}$  and  $c = 96.1 \text{ \AA}$  with  $\beta = 100.4^\circ$ . The triclinic structure has two hexamers and the monoclinic structure one PNP hexamer in the asymmetric unit. Although the space groups are different both of the crystal packings are actually analogous. Namely, hexamers pack next to each other in a planar arrangement that is very approximately hexagonal (Figure 3). This is facilitated by their shape that is roughly hexagonal. This planar arrangement is parallel to  $ab$  plane in the triclinic case (which makes the angle  $\gamma$  very nearly equal to  $120^\circ$ ), and also parallel to  $ab$  plane in the monoclinic case where the ratio of  $a:b = 162.1:93.5 \sim \sqrt{3}$  makes the centered rectangular lattice close to hexagonal. The 3D-structure in both space groups is then realized by stacking of this planar almost hexagonal arrangements on top of each other (Figure 3). The difference between the structures arises from the shear direction and shear angle of stacking between these planes. It is quite conceivable that the relatively poor quality of these crystals is related to the existence of a number of possible directions into which these planes can move with respect to each other (in a manner somewhat reminiscent of a graphite structure).

The single structure that gave rise to very good diffraction data was the one obtained with the crystal that

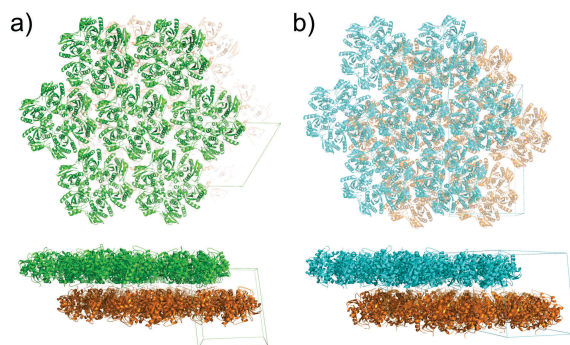


**Figure 3.** Triclinic  $P\bar{1}$  in a) and monoclinic  $C2$  forms in b) of PNP that lead to problematic diffraction datasets. It is clear that irrespective of the different space groups the packing is quite analogous. The hexamers of PNP pack in the approximate planar hexagonal arrangement. The full crystal packing is formed by stacking such planar layers on top of each other (bottom). Different space groups arise by changing the shear angle and direction of the stacking. It is possible that energetic barrier of movement of the layers is relatively low and is causing the disorder which in turn deteriorates the diffraction.

was fished from the crystallization drop where the phosphate was added in 6 steps. The crystal spent approximately 2 hours in the crystallization drop where the final concentration of phosphate was  $12.3 \text{ mmol L}^{-1}$ . This structure crystallized in a monoclinic space group  $P2_1$  with unit cell  $a = 93.3 \text{ \AA}$ ,  $b = 91.5 \text{ \AA}$  and  $c = 93.4 \text{ \AA}$  with  $\beta = 119.9^\circ$ . Details on the crystal structure and refinement are given in Table 1. What can be noted immediately is the similarity of the unit cell to the triclinic structure. In fact, this structure is also isomorphic to the previously described two structures in the sense that the packing in the crystal is realized as the stacking of hexagonal layers. However, as the data in Table 1 confirms, in this case there is no trace of crystal pathologies that were noted in the other structures. This could be the result of longer time that the crystal spent in the soaking solution (2 hours compared to only a 1 minute that the other crystals were soaked), as the crystals had more time to reorder the internal structure which resulted in very good quality of diffraction.

The electron density of the six active sites in the crystal structure reflects the high quality of the dataset (Figure 4). In all six active sites the electron density shows the presence of two imidazole molecules which come from the crystallization solution. They occupy the base binding

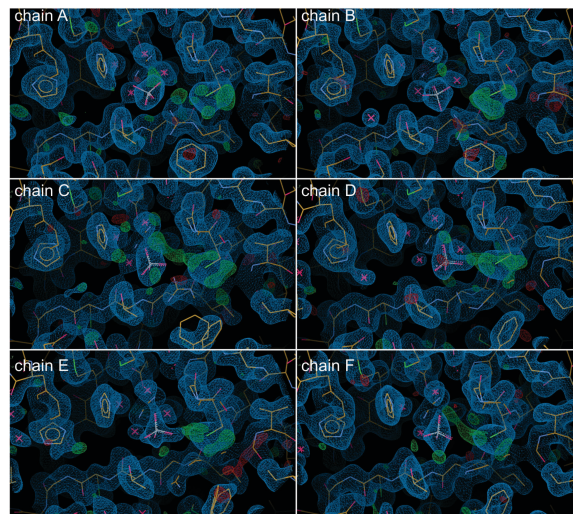


**Figure 4.** Active sites in all six monomers of PNP given in approximately equal orientation. Electron density is shown (blue is  $2mFo-DFc$  map contoured at  $1\sigma$  level, green and red are  $mFo-DFc$  map at  $+3\sigma$  and  $-3\sigma$  levels respectively). In the centre of each panel the phosphate molecules are visible in the map, although not at full occupancy. To the left of each phosphate two molecules of imidazole are visible which are bound in the base binding part of the active site. To the right of each phosphate around Cys19 there is some residual density that corresponds to probable oxidation of cysteine.

part of the active site. Most importantly, the phosphate molecules are visible in the electron density in all six active sites. The occupancies of phosphates are partial, ranging from 0.52 in active site B to 0.64 in active site C. This is in line with generally weaker binding of phosphate to HpPNP compared to e.g. *E. coli* PNP.<sup>[7]</sup> However, somewhat surprisingly, none of the active sites have closed upon phosphate binding, i.e. all the helices H8 in each monomer remained unsegmented. This shows that binding of phosphate alone is not enough to provoke the closing of the active site. One can speculate on the reasons for this in view of the simplest possible setup of this experiment, where the crystals which initially contained no phosphate in the active site, were soaked in phosphate and it was detected in the active site, but it did not cause the closing of at least some active sites. The reason could lie in insufficient concentration of phosphate that resulted in only partial binding and did not trigger the closing. Furthermore, the influence of two imidazole molecules as well as the oxidation of Cys19 in the close proximity to phosphate may also be important (Figure 4). But it could also be a genuine feature of *H. pylori* PNP that perhaps behaves differently than PNPs from other organisms, most notably from *E. coli* PNP. Finally, it may have to do with the complexity of the enzyme mechanism as such, which requires other factors to proceed besides phosphate, such as presence of its other substrate. Also, complex and yet poorly understood cooperativity between monomers has to be kept in mind.

In summary, the present work demonstrates, at least in the crystal form and considering that many external factors influencing phosphate binding have been minimized, that the binding of phosphate to the active site of PNP from *H. pylori* does not cause the conformational change by itself, thus only adding another piece to the puzzle of the sophisticated catalytic mechanism and complex cooperation between subunits of PNPs.

**Acknowledgement.** This work has been fully supported by the Croatian Science Foundation under the project number 7423. We thank the staff at the Elettra synchrotron facility in Trieste, Italy (beamline XRD1), for their support.

## REFERENCES

- [1] P. Malfertheiner, M. Selgrad, J. Bornschein, *Curr. Opin. Gastroenterol.* **2012**, *28*, 608.
- [2] G. Mikleušević, Z. Štefanić, M. Narczyk, B. Wielgus-Kutrowska, A. Bzowska, M. Luić, *Biochimie* **2011**, *93*, 1610.
- [3] Z. Štefanić, M. Narczyk, G. Mikleušević, B. Wielgus-Kutrowska, A. Bzowska, M. Luić, *FEBS Lett.* **2012**, *586*, 967.
- [4] Z. Štefanić, G. Mikleušević, M. Narczyk, B. Wielgus-Kutrowska, A. Bzowska, M. Luić, *Croat. Chem. Acta* **2013**, *86*, 117.
- [5] Z. Štefanić, G. Mikleušević, M. Luić, A. Bzowska, I. Leščić Ašler, *Int. J. Biol. Macromol.* **2017**, *101*, 518.
- [6] G. Koellner, A. Bzowska, B. Wielgus-Kutrowska, M. Luić, T. Steiner, W. Saenger, J. Stepiński, *J. Mol. Biol.* **2002**, *315*, 351.
- [7] M. Narczyk, B. Bertoša, L. Papa, V. Vuković, I. Leščić Ašler, B. Wielgus-Kutrowska, A. Bzowska, M. Luić, Z. Štefanić, *FEBS J.* **2018**, *285*, 1305.
- [8] M. Luić, Z. Štefanić, *Croat. Chem. Acta* **2016**, *89*, 197.
- [9] G. Liechti, J. B. Goldberg, *J. Bacteriol.* **2012**, *194*, 839.
- [10] A. Bzowska, E. Kulikowska, D. Shugar, *Pharmacol. Ther.* **2000**, *88*, 349.
- [11] M. M. Bradford, *Anal. Biochem.* **1976**, *72*, 248.
- [12] E. Gasteiger, C. Hoogland, A. Gattiker, S. Duvaud, M. R. Wilkins, R. D. Appel, A. Bairoch, ed. by John M. Walker, Humana Press, Totowa, NJ, **2005**, pp. 571–607.
- [13] W. Kabsch, *Acta Crystallogr. D. Biol. Crystallogr.* **2010**, *66*, 125.
- [14] A. Vagin, A. Teplyakov, *J. Appl. Crystallogr.* **1997**, *30*, 1022.
- [15] P. D. Adams, P. V Afonine, G. Bunkóczki, V. B. Chen, I. W. Davis, N. Echols, J. J. Headd, L.-W. Hung, G. J. Kapral, R. W. Grosse-Kunstleve, A. J. McCoy, N. W. Moriarty, R. Oeffner, R. J. Read, D. C. Richardson, J. S. Richardson, T. C. Terwilliger, P. H. Zwart, *Acta Crystallogr. D. Biol. Crystallogr.* **2010**, *66*, 213.